

in methylene chloride (3 mL) and added dropwise to the cooled ethyldeneisobacteriochlorin solution. After 20 min of stirring, the flask was transferred directly to a rotavapor and evaporated to dryness. The crude product was purified on alumina (Brockman Grade III, eluting with 3–5% THF/methylene chloride), giving 6 mg (30% yield) of methyl pyropheophorbide **a**, mp 216–218 °C (lit. mp 217–219 °C,<sup>25</sup> 220–225 °C<sup>27</sup>). Vis (relative absorbance): 412 nm (1.00), 506 (0.0879), 538 (0.0814), 608 (0.0744), 666 (0.339). NMR (360 MHz, CDCl<sub>3</sub>): 9.52 (s,  $\beta$ -meso H); 9.40 (s,  $\alpha$ -meso H); 8.55 (s,  $\delta$ -meso H); 8.03 (X of ABX, 2a-H); 6.25 (AB of ABX, 2b- and 2b'-H); 5.20 (AB q, 10-CH<sub>2</sub>); 4.50 (q, 8-H); 4.33 (d, 7-H); 3.72 (q, 4-CH<sub>2</sub>); 3.70 (s, 5-Me); 3.53 (s, 7-OMe); 3.42 (s, 3-Me); 3.25 (s, 1-Me); 2.70, 2.58, 2.30 (each m, 7-CH<sub>2</sub>CH<sub>2</sub>); 1.85 (d, 8-Me); 1.70 (t, 4a-Me).

**Large-Scale Photoreduction in Benzene.** Zinc(II) methyl pyropheophorbide (**7**) (85 mg) was dissolved in 10% ethanol/benzene (100 mL, previously saturated with nitrogen for 20 min). DABCO (1.4 g) and ascorbic acid (880 mg) were added, and the sealed Erlenmeyer flask was irradiated in a Ray-o-net light drum for a total of 18 h with intermittent monitoring of the visible spectrum. The product was poured into ether (200 mL) and water (100 mL) and separated. The organic layer was washed with water (4–5 times), dried, and evaporated to dryness. The product was purified by preparative TLC (3% methanol/methylene chloride) using two plates. Crystallization from methylene chloride/*n*-hexane gave 45 mg of blue solid. **Zinc(II) 2-Vinylisobacteriochlorin (15)**, mp > 250 °C. Vis: 382 nm ( $\epsilon$  50 600), 394 (48 100), 412 (47 300), 484 (7000), 554 (12 100), 600 (27 800), 650 (5700). NMR (360 MHz,

CDCl<sub>3</sub> and pyridine-*d*<sub>5</sub>): see Table I.

**Zinc(II) 2-Vinylrhodoisobacteriochlorin (27).** This reduction was done by the large-scale procedure using 22 mg of zinc(II) rhodochlorin (**26**), 700 mg of DABCO, and 400 mg of ascorbic acid in 50 mL of 10% ethanol/benzene. All the starting material had been completely consumed in 1 h, after which the reaction was worked up as in the previous reaction. Separation was achieved by preparative TLC (1.5% methanol/methylene chloride), and the product was obtained as a solid from *n*-hexane. Vis: 388 nm ( $\epsilon$  58 000), 402 (60 600), 518 (4900), 592 (29 100), 638 (7000). NMR (360 MHz, CDCl<sub>3</sub> and pyridine-*d*<sub>5</sub>): 8.62, 8.49 (s,  $\beta$ - and  $\delta$ -meso H); 7.31, 7.30 (s,  $\alpha$ -meso H); 6.68 (s,  $\delta$ -meso H); 6.20 (m, 2a-H); 5.40 (m, 2b- and 2b'-H); 4.68 (m, 2-H); 4.25, 4.10, 3.75, 3.63 (m, 1-, 7-, and 8-H, 6a-OMe); 3.60, 3.59 (s, 7d-OMe); 3.35 (q, 4a-CH<sub>2</sub>); 3.27 (s, 5-Me); 2.76 (s, 3-Me); 2.25 (m, 7-CH<sub>2</sub>CH<sub>2</sub>, impurity?); 1.50 (m, 1- and 8-Me, 4b-Me).

**Zinc(II) 2-Ethylisobacteriochlorin (32).** Using the large-scale procedure 19 mg of zinc(II) mesorhodochlorin (**30**) was irradiated for 24 h with 800 mg of DABCO and 400 mg of ascorbic acid in 50 mL of 8% ethanol/pyridine. Purification of the reduced product was not possible as the product appeared to oxidize on silica gel. The crude product was obtained as a solid from *n*-hexane. Vis (relative absorbance of crude product): 395 nm (1.00), 554 (0.160), 594 (0.443), 630 (0.109) (chlorin impurity?). NMR (360 MHz, CDCl<sub>3</sub> and pyridine-*d*<sub>5</sub>): 8.80, 7.704, 7.701 (s,  $\alpha$ -,  $\beta$ -, and  $\delta$ -meso H); 7.06, 7.01 (s,  $\gamma$ -meso H); 4.72 (m, 6-H); 4.62 (m, 5-H); 4.00–2.95 (m, 7- and 8-H, 1- and 3-Me, 6a- and 7d-OMe, 2a- and 4a-CH<sub>2</sub>); 2.20 (m, 7-CH<sub>2</sub>CH<sub>2</sub>, impurity?); 1.80–1.50 (m, 5- and 8-Me, 2b- and 4b-Me).

**Acknowledgment.** This research was supported by a grant from the National Science Foundation (Grant CHE 86-19034).

(27) Fischer, H.; Orth, H. *Die Chemie des Pyrrols*; Akademische Verlag: Leipzig, 1940; Vol. II, part 2, p 74.

## Lipid Bilayer Fibers from Diastereomeric and Enantiomeric *N*-Octylaldonamides

Jürgen-Hinrich Fuhrhop,\*† Peter Schnieder,†‡ Egbert Boekema,† and Wolfgang Helfrich§

Contribution from the Institut für Organische Chemie der Freien Universität Berlin, Takustrasse 3, 1000 Berlin 33, Federal Republic of Germany, Fritz-Haber-Institut der Max-Planck-Gesellschaft, Faradayweg 4-6, 1000 Berlin 33, Federal Republic of Germany, Abt. Elektronenmikroskopie, and the Institut für Physik der Freien Universität Berlin, Arnimallee 22, 1000 Berlin 33, Federal Republic of Germany. Received August 7, 1987

**Abstract:** The aggregation behavior of eight diastereomeric *N*-octylaldonamides, three enantiomers (galacton, mannnon, glucon), and corresponding racemates was investigated mainly by electron microscopy. Head groups with a sterically undisturbed all-anti conformation (galacton, mannnon) lead to "whisker"-type aggregates, which appear as rolled up, bilayer sheets in both aqueous and 1,2-xylene gels. One pair of 1,3-syn-positioned OH groups in the all-anti conformation neighboring on the amide group, lead to extremely thin helical whiskers of high curvature in water (glucon) or 1,2-xylene (talon). If the outer OH groups are in syn positions in the all-anti chain conformations, the *N*-octylamides become highly water-soluble (allon, altron, idon) and form rolled up, bilayer sheets in 1,2-xylene (gulon). The length-to-diameter ratios in the aggregates are often higher than 10<sup>4</sup>. The fibers are stabilized by amide hydrogen bonds and/or the hydrophobic effect. They can be conceived as models for prebiotic assemblies, which may lead to condensation biopolymers in aqueous media.

Hydrophobic bilayers with well-defined morphologies may serve (i) as structural models for biological membranes and (ii) as scaffolds for synthetic functional systems. So far, spherical vesicles<sup>1</sup> and fibers<sup>2–7</sup> have been obtained, the latter being either ribbons or tubes. If composed of chiral molecules, the ribbons are usually twisted or helically wound.<sup>5,6</sup> In a first survey on relationships between molecular structures of several synthetic amphiphiles and their nonspherical aggregates, Kunitake singled out the interaction of linear and bent aromatic rigid segments as the most important elements.<sup>2</sup> We explained the helicity of

elongated bilayers made from chiral molecules by involving spontaneous torsion of the edges<sup>8</sup> and traced fibrous aggregates<sup>9</sup>

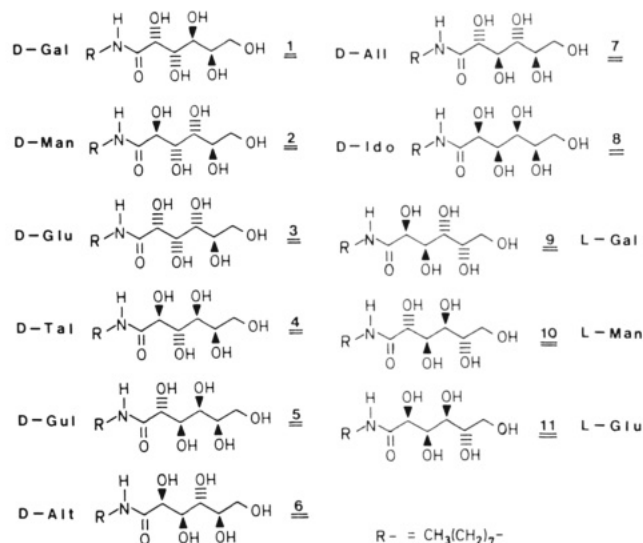
- (1) Fendler, J. H. *Biomimetic Membranes*; Wiley, New York, 1982.
- (2) Kunitake, T.; Okahata, Y.; Shimomura, M.; Yasunami, S.; Takarabe, K. *J. Am. Chem. Soc.* **1981**, *103*, 5401–5413.
- (3) Papahadjopoulos, D.; Vail, W. J.; Jacobson, K.; Poste, G. *Biochim. Biophys. Acta* **1975**, *394*, 483–491.
- (4) Tachibana, T.; Yoshizumi, T.; Hori, K. *Bull. Chem. Soc. Jpn.* **1979**, *52*, 34–41.
- (5) Nakashima, N.; Asakuma, S.; Kunitake, T. *J. Am. Chem. Soc.* **1985**, *107*, 509–510.
- (6) Pfannemüller, B.; Welte, W. *Chem. Phys. Lipids* **1985**, *37*, 227–240.
- (7) Yager, P.; Schoen, P. E.; Davies, C.; Price, R.; Singh, A. *Biophys. J.* **1985**, *48*, 899–906.
- (8) Helfrich, W. *J. Chem. Phys.* **1985**, *85*, 1085–1087.

\* Institut für Organische Chemie der Freien Universität Berlin.

† Fritz-Haber-Institut der Max-Planck-Gesellschaft.

§ Institut für Physik der Freien Universität Berlin.

Chart 1



from *N*-alkyl-D- and -L-gluconamides back to formation of chains of amide hydrogen bonds. They can be regarded as substitutes of the rigid aromatic components of Kunitake's compounds. It was also shown that the racemic compound formed platelets rather than micellar fibers ("chiral bilayer effect").<sup>9</sup> We report here on eight diastereomeric *N*-octyl-D-aldonamides which produce "whisker-like" helices, tubes, or ribbons or do not aggregate at all. Simple relationships between the head group's stereochemistry and the aggregate morphologies have been found.

## Results

The eight diastereomeric aldonamides **1–8** and three enantiomers **9–11** listed in Chart 1 were obtained by electrolytic oxidation of the corresponding hexoses to the lactones and amidation with octylamine.<sup>10,11</sup>

Galactonamides **1** and **9** were the least soluble of the eleven compounds. Saturated aqueous solutions (0.4–0.5% w/v) were obtained by refluxing the D-enantiomer. On cooling to room temperature, the solution solidified to a gel. Fibers with diameters of about 100 nm and a length of several  $\mu\text{m}$  or more were observed on electron micrographs (Figure 1a), whereby the solution was cooled rapidly. The narrow fibers made from pure D- and L-enantiomers appeared as ribbons and were sometimes twisted. The D-enantiomer produced a left-handed twist and the L-enantiomer a right-handed twist (Figure 1 (parts b and c)). Slow cooling resulted not in fibers but in ill-defined microcrystallites. At branching points, the rapidly grown fibers often lay orthogonal to each other (Figure 1a).

The racemic mixture of **1 + 9** was even less soluble than the pure enantiomers. It also formed fibers but without branchings which would be expected for fast growing dendritic crystals.<sup>12</sup> There is obviously never enough material in the dilute solutions to allow the formation of ramifications. The racemic fibers are usually wider by a factor of 10 and appear to be collapsed tubes (Figure 1d).

All gels made from galactonamides were of low tensile strength because of the low fiber concentration and were stable for several weeks. Over several months precipitation occurred. No organogels were formed in 1,2-xylene, since galactonamides were insoluble in this solvent even after prolonged refluxing.

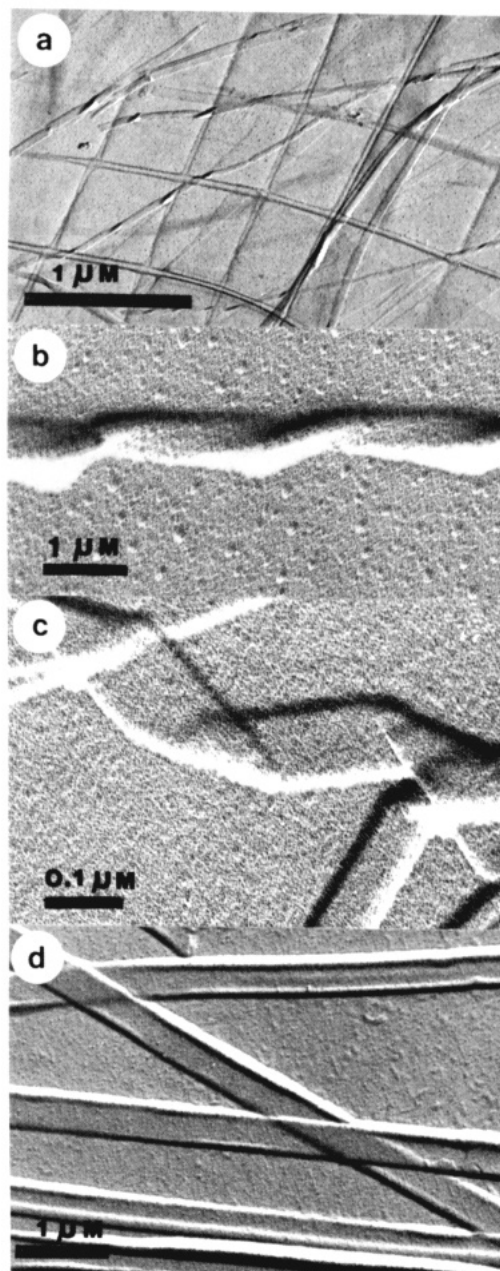


**Figure 1.** Electron micrographs of aggregate fibers in gels made from *N*-octylgalactonamides in water (Pt/C shadowing): (a) D-galactonamide **1**; overall view; (b) left-handed twist in ribbons made from D-galactonamide **1**; (c) right-handed twist in L-galactonamide **9** ribbons; and (d) tubes from racemic **1 + 9**.

*N*-octyl-D-mannonamide **2** was more water-soluble than the galacton diastereomer by about a factor of 5–10. Solutions (3%, w/v) were formed in boiling water and solidified to a white gel, on cooling to room temperature. Electron micrographs showed multilayer cylinders (Figure 2a–c). Freeze etching of these cylinders (or "cochleae")<sup>3</sup> revealed several bilayers rolled up around a hollow center (Figure 2d), and vesicles were often adsorbed to the surface (Figure 2c). In boiling 1,2-xylene, the mannonamide **2** gave viscous dispersions which did not solidify at room temperature. Nevertheless, electron micrographs showed regular multilayer cylinders very similar to those in the aqueous gels. They looked like cigars, the edges of the sheets making angles of 45° with the long axis. By measuring the difference in diameter between different parts of the vesicular cylinders and counting the decrease in number of sheets between these points, the thickness of one sheet could be estimated to be  $39 \pm 2 \text{ \AA}$ . This corresponds to the length of a molecular bilayer of **2** in the all-anti conformation (Figure 2e). Both gels in water as well as in xylene were stable for weeks. The racemic mixture of **2 + 10** does not

(9) Fuhrhop, J.-H.; Schnieder, P.; Rosenberg, J.; Boekema, E. *J. Am. Chem. Soc.* **1987**, *109*, 3387–3390.

(10) Zabel, V.; Müller-Fahrnow, A.; Hilgenfeld, R.; Saenger, W.; Pfannmüller, B.; Enkelmann, V.; Welte, W. *Chem. Phys. Lipids* **1986**, *39*, 313–327.

(11) Emmerling, W. N.; Pfannmüller, B. *Makromol. Chem.* **1978**, *179*, 1627–1633.

(12) Saratorkin, D. D. *Dendritic Crystallisation*; Consultants Bureau, Inc.: New York, 1959.

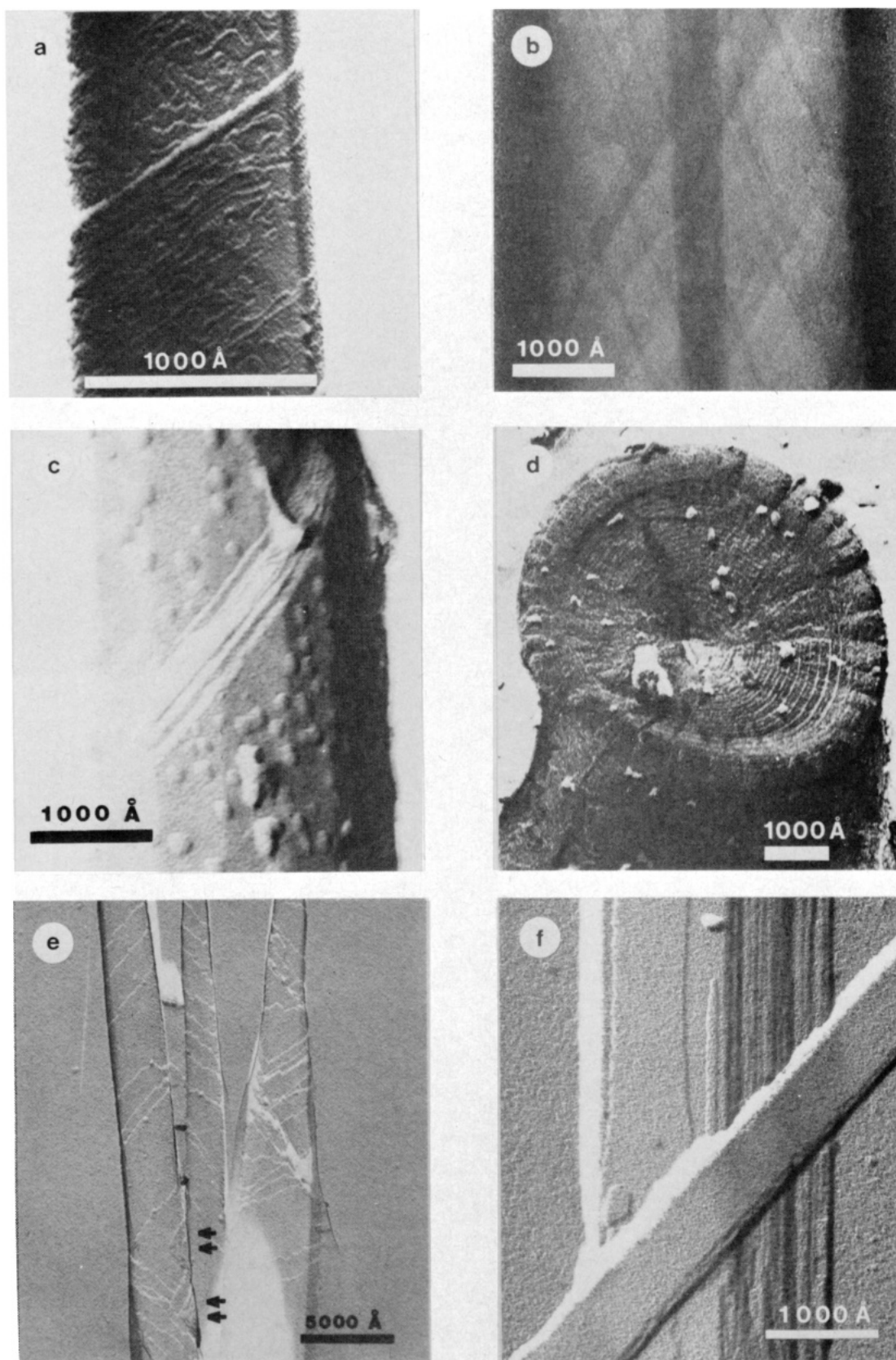


**Figure 2.** Electron micrographs of mannonamide aggregates from water (a–e) or xylene (f): (a and b) details of aged fiber aggregates of D-mannonamide **2**; negatively stained with phosphotungstate (b) or shadowed with Pt/C (a); (c and d) similar fibers after freeze etching and Pt/C shadowing; (e) cigarlike tubes of D-mannonamide **2** in xylene; the arrows indicate corner of sheets (Pt/C shadowing); (f) platelets from racemic mannonamide **2** + **10** in water (Pt/C shadowing).

produce fibers. The platelets which were found instead (Figure 2), probably consist of strongly hydrated bilayers, since the material is very soft.

The gluconamide **3** is well-soluble in boiling water ( $\approx 50\%$  w/v). The hot aqueous solutions solidified to a gel on cooling, in the

concentration range of 0.5–50% (w/v). Electron micrographs of the fibers in the aqueous gels have already been published.<sup>6,9</sup> Figure 3a gives a typical example of an aged gel which contains helices of unknown multiplicity. In the presence of phosphotungstate at pH 2 or 7, helical ropes of the minimal thickness of

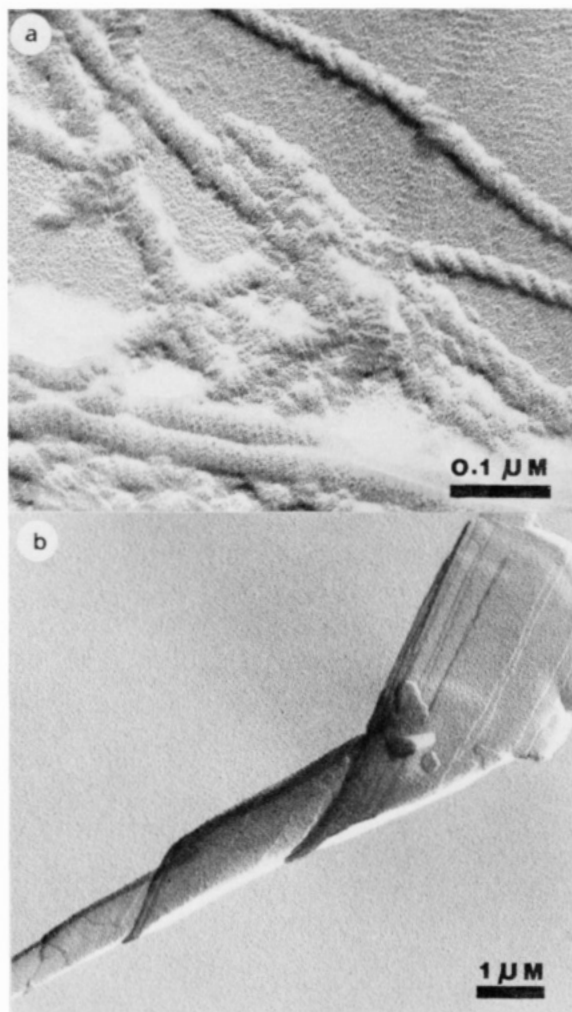


**Figure 3.** Electron micrographs of fiber aggregates of gluconamide **3**: (a) from water and (b) from xylene (Pt/C shadowing).

a molecular bilayer were also obtained.<sup>9</sup> In 1,2-xylene gels, vesicular cylinders were seen which often showed the rolling up of multilayer sheets (Figure 3).

The aqueous gels and organogels from gluconamides were less stable than those made from galactonamides and mannonamides. Anhydrous crystals usually separated out within days. The crystal structure of the pure enantiomers showed head-to-tail arrangements.<sup>10</sup> The racemate (**3** + **11**) again did not form fibers in water but precipitated quickly from hot solutions in the form of platelets without curvature.<sup>9</sup> The X-ray structure of the racemate is not known.

The talonamide **4** has roughly the same solubility as the gluconamide diastereomer. It formed unstable gels in water, containing short and fragile fibers (Figure 4a). The fast grown organogel fibers were uniformly long and looked like well-developed whiskers (Figure 4b). In less rapidly cooled xylene gels, helical rods were sometimes detected (Figure 4c). The xylene gel was stable for several days, and from the aqueous gels, ill-defined crystals were rapidly formed.

The final compact gel was formed by D-gulonamide **5** in 1,2-xylene. Tubes from rolled up sheets were usually accompanied by platelets composed of bilayers (Figure 5). From hot aqueous solutions, **5** crystallized immediately on cooling.

The diastereomers **6–8** did not form gels or viscous solutions. They were all very soluble in cold water.

<sup>1</sup>H NMR spectra of the D-gluconamide **3** in hot deuterium oxide ( $\geq 75^\circ\text{C}$ ) gave well-resolved signals which were indistinguishable from those of monomolecular methanolic solutions. Vesicles were therefore not present in the hot solutions. Galactonamides and mannonamides behaved similarly. Infrared spectra of **3** in D<sub>2</sub>O also showed the expected differences: the amide II band at 1460

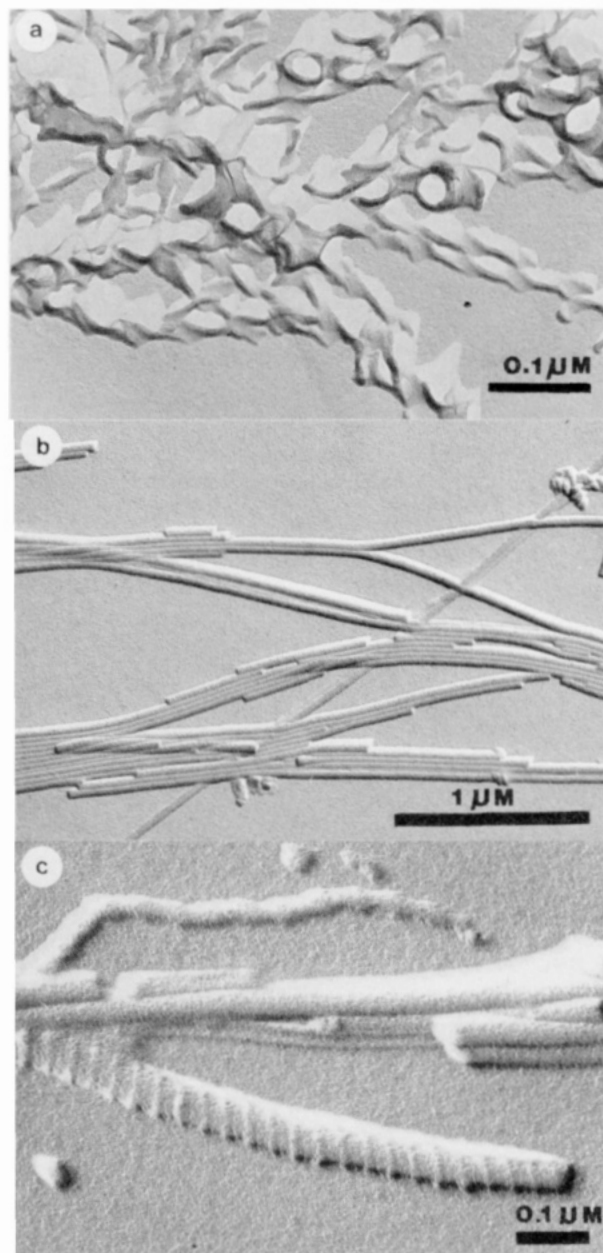


**Figure 4.** Electron micrographs of D-talonamide **4** aggregates: (a) from water, and (b and c) from xylene (Pt/C shadowing).

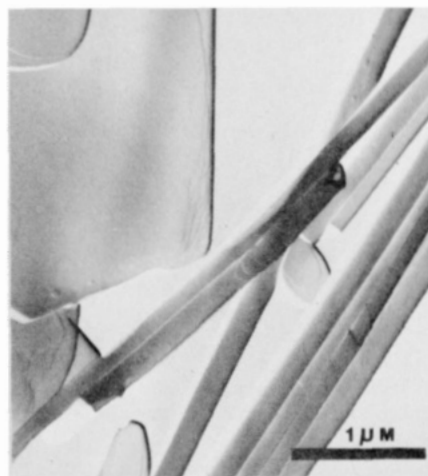


**Figure 5.** Electron micrograph of gulonamide **5** aggregates in 1,2-xylene (Pt/C shadowing).

$\text{cm}^{-1}$  was of much higher intensity at  $25^\circ\text{C}$  (gel) than at  $75^\circ\text{C}$  (solution), and the bands above  $2500\text{ cm}^{-1}$  are much broader in



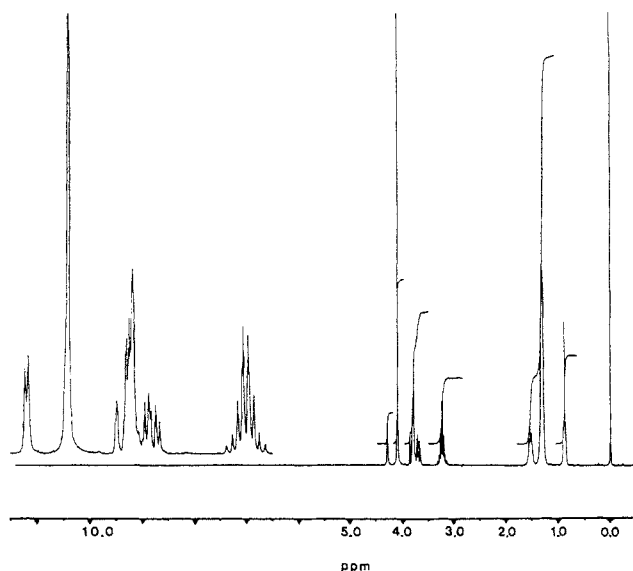


Figure 6.  $^1\text{H}$  NMR spectrum of gluconamide 3 micelles<sup>6</sup> at  $\geq 75^\circ\text{C}$  in  $\text{D}_2\text{O}$ .

the gel. The latter phenomenon has also been observed in gelatin sols and gels.<sup>13</sup>

### Discussion

The fibrous aggregates are conceived as single crystals or sometimes polycrystals with high, length-to-diameter ratios. Such filaments are usually depicted as "whiskers" in the literature.<sup>14a-c</sup> The best known whiskers are made of ceramics or metals and are usually formed in electrolyses or condensation processes. Ribbon-structures and scroll-structures, which look similar to those in Figures 1 and 2 were, for example, obtained by sublimation of graphite at 3900 K and a pressure of 92 atmospheres of argon.<sup>14</sup> Helical structures similar to those in Figures 3 and 4 were observed in metal whiskers which were made by reduction of metal halides at high temperatures.<sup>14b,c</sup> The high degree of crystal perfection found in the cylindrical graphite whiskers has been rationalized with the assumptions of near equilibrium conditions and molecular aggregates in the vapor phase at the high temperatures and pressures applied. Firstly, thin graphite sheets ( $\leq 100$  nm) were formed, coiled up to reduce surface energy and then thickened by tangential growth in spiral fashion along screw dislocations.<sup>14c</sup> Similar sequences of events should occur in the formation of helical metal whiskers. The screw sense of the individual helices will be equally or righthanded.

The crystallization processes in the formation of micellar lipid fibers could also be similar to those proposed for ceramic and metal whiskers. We assume that the aldonamides occur as spherical micellar aggregates in hot aqueous solutions. Pfannmüller et al.<sup>6</sup> determined a cmc at  $90^\circ\text{C}$  ( $1.0 \cdot 10^{-2}$  molar) for the gluconamide 3. These micelles should rearrange to small planar or rolled up sheets, when the temperature is low enough to allow the cooperative formation of amide hydrogen bond chains. These sheets grow to whiskers as the solution becomes (i) highly supersaturated on quick cooling and (ii) is rapidly depleted of solutes by the loss of micellar clusters. The high degree of perfection found in some of the lipid bilayer whiskers (e.g., Figure 4b) again points to near equilibrium conditions at the gelation point.

The solvophobic bilayer whiskers described in this paper offer three interesting structural features: (i) they can be obtained in large quantities in gels at moderate temperatures; (ii) ultrathin fibers (diameters  $\leq 10$  nm) are produced by gluconamides in water or by talonamides in 1,2-xylene; and (iii) the chirality of the helices is predetermined by the structure of the chiral monomers.

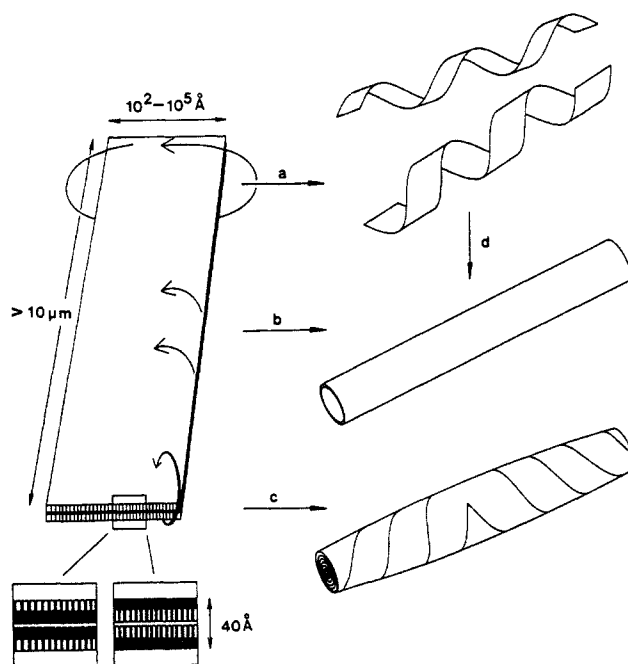


Figure 7. Twisting (a) or rolling up (b and c) of planar bilayer sheets around corners (c) or edges (a and b) to yield helices, tubes, or cigarlike scrolls.

Amphiphiles 1 and 2 with no 1,3-syn hydroxy groups favor a nondisturbed, all-anti conformation of the carbon chain. A stretched conformation is expected for these molecules and a noncurved bilayer aggregate should prevail. The very long and uniform ribbons displayed by these aldonamide aggregates are probably whiskers which grow with the screw dislocations which they enclose. Screw dislocations can occur even in a single bilayer between the monolayer lattices and are presumably caused by interlayer interactions of the hydroxyl groups. Ribbons could alternatively also result from a highly anisotropic energy per unit length of the bilayer edges. Such anisotropies can be caused in our crystals by amide hydrogen bonds, which should be arranged in straight or slightly curved parallel lines. However, the fact that irregular platelets were formed at low cooling rates instead of ribbons is more consistent with whiskers. The bending elasticity of the bilayers also appears to be isotropic as indicated by gradient angles of helically wound ribbons near  $45^\circ$ .<sup>8</sup> Likely mechanisms of ribbon windings are summarized in Figure 7.

The micellar cylinders and helices produced by gluconamides 3, 11, and talonamide 4 are most probably caused by a bend in the head group regions. This bend was found in crystal structures of corresponding polyols<sup>17,18</sup> and is caused by 2,4-syn interactions of the hydroxyl groups leading to a relative broadening of the head group region. The estimated ratio of diameters head group to hydrophobic chain is about 1.5 (1.48) and is consistent with data for other micellar aggregates.<sup>19</sup> The thickness of one micellar disk can be estimated from the volume of the enclosed methylene groups ( $24 \times 17 \times 8 \text{ \AA}^3$ ) and should be about 9–10 Å.

The amphiphiles 5–8 which are highly water soluble and do not form aqueous gels all contain syn-oriented hydroxyl groups on C (3) and C (5). The most stable conformation of these aldonamides is obviously bent in such a way that the formation of a regular amide hydrogen bond chain is prevented by extensive hydration. Figure 9 reproduces three typical crystal structures

(15) Berman, H. M.; Jeffrey, G. A.; Rosenstein, R. D. *Acta Crystallogr., Sect. B: Struct. Crystallogr. Cryst. Chem.* **1968**, *B24*, 442–449.

(16) Arzania, N.; Jeffrey, G. A.; Shen, M. S. *Acta Crystallogr., Sect. B: Struct. Crystallogr. Cryst. Chem.* **1971**, *B28*, 1007–1013.

(17) Park, J. Y.; Jeffrey, G. A.; Hamilton, W. C. *Acta Crystallogr., Sect. B: Struct. Crystallogr. Cryst. Chem.* **1971**, *B27*, 2393–2401.

(18) Horton, Z.; Walaszek, Z.; Ekiel, I. *Carbohydr. Res.* **1983**, *119*, 263–268.

(19) Eibl, H. *Angew. Chem., Int. Ed. Engl.* **1984**, *23*, 257f.

(13) Milch, R. A. *Nature (London)* **1964**, *202*, 84–85.

(14) (a) Brenner, S. S. *Acta Met.* **1956**, *4*, 62–70. (b) Edwards, P. L.; Svager, A. J. *Appl. Phys.* **1964**, *35*, 421–423. (c) Bacon, R.; *J. Appl. Phys.* **1960**, *31*, 283–290.

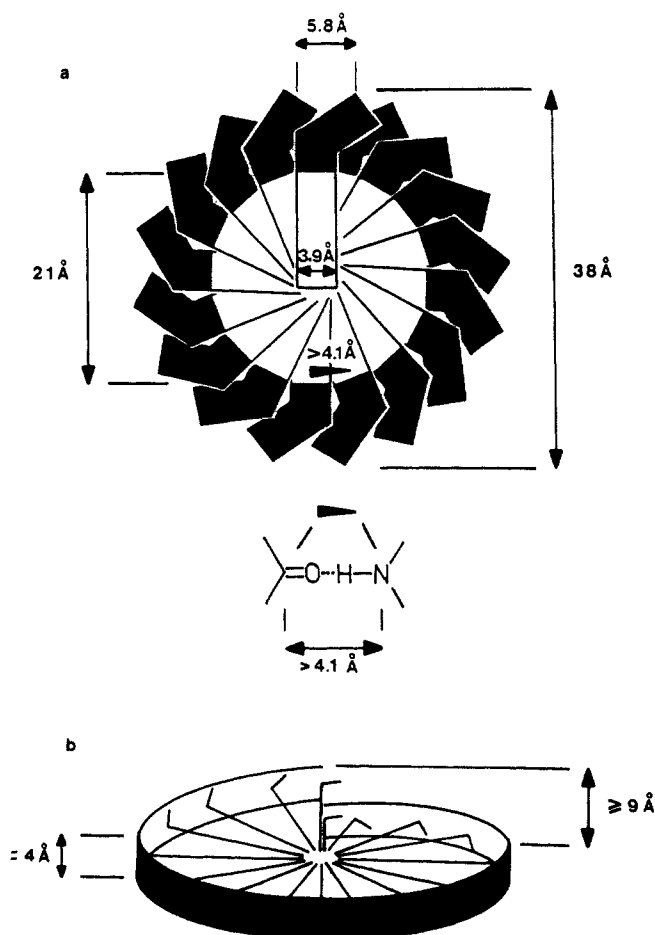


**Figure 8.** (a) Top view of a micellar disk of a cylinder ("bulgy helix")<sup>10</sup> made of gluconamide **3**. **3** is drawn in a bend conformation (see Figure 9); (b) neighboring amphiphiles as connected by amide hydrogen bonds.

of a nondisturbed straight chain polyol and a bent as well as a highly irregular diastereomer, which illustrate the argument.

Another important aspect in the stereochemistry of aldonamide aggregates is the presence of enantiomers. In all racemic mixtures tried, namely galactonamides **1** + **9**, mannnonamides **2** + **10**, and gluconamides **3** + **11**, the solubility in hot water was lowered by factors of about three to five, as compared to the pure enantiomers. The mannnonamides and gluconamides precipitated, on the cooling of the hot solution, as platelets. No stable gel was formed. This behavior is rationalized with a "chiral bilayer effect", which leads to rapid formation of crystalline bilayer sheets in racemates, whereas pure enantiomers rearrange slowly to enantiopolar (or head to tail) sheets.<sup>9</sup> The galactonamide racemate, however, gave stable gels which contained long tubes instead of platelets (Figure 1d). The explanation for the extraordinary stability of these racemic whiskers with the low solubility of the galactonamide in cold water is, that the rapidly formed whiskers presumably cannot rearrange to multilayered sheets because the equilibrium concentration of micelles in solution is too low.

In the 1,2-xylene gels, the stereochemical differences between the polar groups are not as important as in aqueous gels. All aldonamides are either insoluble or form bilayer scrolls. It is not known whether the aldon groups lie outside or within the bilayer sheets. The missing stereochemical differentiation in xylene, as compared to water, can be related to a lack of solvation of the polar groups. In xylene, the all-trans conformation of every aldonamide predominates in the same way as in water-free crystals of gluconamides.<sup>10,20</sup> Only extensive hydration of the outer hydroxyl groups which are attached to crystalline sheets of oli-

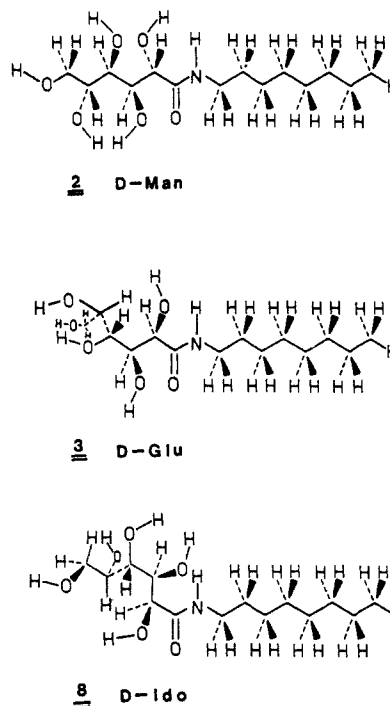


**Figure 9.** Examples for an undisturbed straight-chain aldonamide, namely **2**, an aldonamide with a bend (**3**), and a highly irregular chain conformation (**8**). The given conformations are based on crystal structures of the corresponding alditols<sup>15-17</sup> and related conformational studies in solution.<sup>18</sup>

gomethylene chains leads to disturbances of the all-trans conformations.

## Conclusion

Solubilities and aggregate structures of aldonamide **1-11** depend directly on the stereochemistry of the polyol head groups. Undisturbed all-anti chains lead to bimolecular sheets; a bend close to the amide group produces cylindrical micelles with high curvature, and a twist at the end of the chain causes water solubility of the amphiphiles and prevents fiber formation. The last result is in qualitative agreement with Kunitake's statement that "too much bending... is not advantageous for molecular ordering".<sup>2</sup> A little bending, on the other hand, leads to ultrathin aggregates with high curvature and low tendency to sheets formation. A rigid segment is clearly not needed, in order to produce stable fibers.

The structural principles outlined in this paper for *N*-octylaldonamides need to be tested with other stereoisomeric fibers. Another example for the "chiral bilayer effect", namely D-polylysine and L-polylysine, has been published.<sup>21</sup> Work on amphiphiles with cyclic carbohydrate head groups is in progress. It is also tempting to assume that the chiral fiber aggregates may be useful as substrates for condensation polymerization in aqueous media.

## Experimental Section

**General Methods.** Electron microscopy was carried out with a Philips EM 300 at 80 KV. Freeze etching was carried out with a Balzers freeze etching unit. <sup>1</sup>H NMR spectra were recorded on a Bruker WH 270 MHz spectrometer. A Perkin-Elmer DSC-2C calorimeter and large pans were used for differential scanning calorimetry.

**Syntheses of *N*-1-Octylaldonamides.** Aldonic acid lactones were either purchased (Sigma) or prepared by indirect electrochemical oxidation of the corresponding hexoses in the presence of calcium bromide. Excess bromide was precipitated with silver carbonate and filtered off. The solution was then stirred with a strongly acidic ion exchange resin (Merck) and dehydrated by azeotropic distillation with 1-butanol. Aminolysis of the lactones (to give amides **1-11**) was performed by heating

(20) Müller-Fahrnow, A.; Zabel, V.; Steifa, M.; Hilgenfeld, R. *J. Chem. Soc., Chem. Commun.* **1986**, 21, 1573-1574.

(21) Fuhrhop, J.-H.; Krull, M.; Büldt, G.; *Angew. Chem.* **1987**, 99, 707-708.

with equimolar amounts of octylamine in methanol.

All products were crystallized or precipitated from methanol. All products gave satisfactory spectra (IR,  $^1\text{H}$  NMR, mass spectra, chemical ionization). Satisfactory elemental analysis were only obtained from compounds 1-5 and 9-11. The idon-, allon-, and altronamides did not solidify, and carbon values were low.

**Gelation Procedures.** **A. Hydrogels.** (i) **Galactonamides.** 1 (50 mg) was dissolved in 10 mL of boiling water and cooled in an ice bath. A turbid gel of low mechanical strength was formed within a few seconds and did not change its appearance after 3 months. Slow cooling did not produce gels but flaky precipitates. Concentrations greater than half a percent (w/v) could not be obtained; lower concentrations gave even less solid gels. The racemate, 1 + 9, was less soluble ( $\approx 30$  mg/10 mL) and formed also stable gels of low tensile strength.

(ii) **Mannonamides.** 2 or 10 (100 mg) was dissolved in 10 mL of refluxing water and again cooled with an ice bath. Solidification to a white gel of medium mechanical stability occurred within a few seconds. Concentration of up to 300 mg in 10 mL of hot water could be obtained. Concentrations below 0.5% (w/v), or slow cooling, resulted in flaky precipitates. The racemate (100 mg/10 mL) 2 + 10 gave a white gel on rapid cooling, which behaved similarly to the gels from the pure enantiomers.

(iii) **Gluconamides.** 3 or 11 (100 mg) was dissolved in 10 mL of water on heating to 75 °C. The solutions were then left standing, and a compact, clear gel was formed within 2-3 min. After about 30 min, the gels became turbid, and crystals formed within a few days. This sequence of events appeared in a concentration range of 0.5-50% (w/v). The racemate 3 + 11 dissolved only above 85 °C and precipitated on cooling. The solubility of the racemate in boiling water is of the same order as for the enantiomers.

(iv) **Talonamide.** 4 (100 mg) was dissolved in 2 mL of water at 60 °C. A clear, solid gel was formed within a few minutes at room temperature, but crystals appeared rapidly. The concentration range for formation of gels was 0.5-70% (w/v).

(v) **Gulonamide.** The solubility of 5 in boiling water was higher than 100% (w/v). No gelation was observed. **B. Organogels.** (i) **Galactonamides.** 1 and 9 were practically insoluble in refluxing xylene. (ii) **Mannonamides.** 2 or 10 (100 mg each) was dissolved in 20 mL of refluxing 1,2-xylene and cooled in an ice bath. Viscous and turbid solutions were obtained, which did not solidify or produce precipitates. From xylene solutions of racemic 2 + 10 precipitated white flakes on

cooling. 1,3-Xylene did not work because its boiling point is slightly too low to dissolve 2. (iii) **Gluconamides.** 3 or 11 (100 mg) was dissolved in 10 mL of refluxing 1,2-xylene and cooled to room temperature. Clear, compact gels were obtained from which crystals precipitated within 3 or 4 days. The useful concentration range for the formation of clear gels was 1-7% (w/v). The racemate 3 + 11 behaved identically with the pure enantiomers.

(iv) **Talonamide.** 4 (50 mg) was dissolved in 50 mL of 1,2-xylene at 100 °C. A clear, compact gel was obtained on cooling. Crystallization occurred only after days. The concentration range for gelation was 1-100% (w/v).

(v) **Gulonamide.** Similar behavior to talonamide.

**Electron Microscopy Grids.** Carbon-coated copper grids were dipped into freshly prepared gels or hot viscous solutions (talonamide in water, mannonamide in xylene). The samples were shadowed with platinum-carbon at an elevation angle of about 30° with an Edwards coating system E 306A. Negatively stained gels (e.g., Figure 2b) were prepared with 2% (w/v) phosphotungstic acid. The pH was adjusted to 7 with sodium hydroxide. In order to determine the handedness of helix or ribbon twistings, great care was taken in exposing heavy metal-shadowed surfaces directly to the electron beam.

Freeze etching (Figure 2 (parts c and d)) was carried out with a Balzer BA 360 freeze-etching device. A small droplet of freshly prepared 3% hydrogel of 2 without any cryoprotectants was mounted on a specimen support. It was rapidly immersed into liquid Freon A 13 (Messer-Griesheim) cooled by liquid nitrogen. The probe was fractured at 173 K in vacuo in small steps down to a final depth of about 40 nm. This was followed by etching at 173 K for 30 s. Immediately thereafter, the etched surface was shadowed with platinum-carbon at an elevation angle of 30°. Subsequently it was covered by a layer of pure carbon at an elevation angle of 90°. The replica was floated off from the specimen support and loaded onto a copper grid. Electron microscopy was carried out with a Siemens Elmiskop 1 at a direct magnification of 40 000.

**Acknowledgment.** This work was supported by the Deutsche Forschungsgemeinschaft (SFB 312 "Gerichtete Membranprozesse"), the FNK of the Freie Universität Berlin, and the Fonds der Chemischen Industrie. We thank Prof. E. Zeitler for his continuous interest and help.

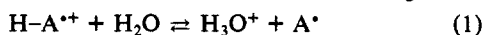
## Acidities of Radical Cations Derived from Remotely Substituted and Phenyl-Substituted Fluorenes

Frederick G. Bordwell,\* Jin-Pei Cheng, and Mark J. Bausch

Contribution from the Department of Chemistry, Northwestern University, 2145 Sheridan Road, Evanston, Illinois 60208. Received June 29, 1987

**Abstract:** Estimates of the acidities of the radical cations derived from remotely substituted and phenyl-substituted fluorenes have been made from measurements of the acidities and oxidation potentials of the fluorenes and the oxidation potentials of their conjugate bases. The radical cation acidities of fluorene, 2-bromofluorene, and 4-azafuorene were all estimated to be -17. The  $\text{p}K_{\text{HA}^{\bullet+}}$  values for fluorenes bearing remote donor substituents were as follows: 3-Me (-15); 2-Me (-15); 3-MeO (-13.5); 2-PhS (-12); 3,6-(MeO)<sub>2</sub> (-12); 2-MeO (-10); 2,7-(PhS)<sub>2</sub> (-9.5); 2,7-(MeO)<sub>2</sub> (-6); 2,3,6,7-(MeO)<sub>4</sub> (-2); 2-Me<sub>2</sub>N (+1). A plot of  $E_{\text{ox}}(\text{HA})$  for the fluorenes vs the acidities of the corresponding radical cations,  $\text{p}K_{\text{HA}^{\bullet+}}$ , is linear (slope = 0.93;  $R^2 = 0.995$ ). The introduction of a phenyl or aryl group into the 9-position of fluorene, as in 9-Ph, 9-*p*-tolyl, 9-*m*-ClC<sub>6</sub>H<sub>4</sub>, or 9-mesitylfluorenes and fluoradene, increased the radical cation acidity ( $\text{p}K_{\text{HA}^{\bullet+}} = -21$  to  $-23$ ). A similar Ph effect was observed on the acidities of 2,7- or 3,6-dimethoxyfluorene radical cations. These acidity increases are associated with decreases in the 9-C-H bond dissociation energies (BDEs) of 4-9 kcal/mol, relative to that of fluorene. On the other hand, fusion of a benzene ring onto the 1,2- or 2,3-positions lowers the acidity of fluorene by 6 and 5  $\text{p}K_{\text{HA}^{\bullet+}}$  units, respectively, an effect which overshadows the small acid-strengthening effects caused by the  $\sim 1$  kcal/mol lower 9-C-H BDEs.

The acidities of only a few radical cations have been determined because of the difficulty in measuring the position of an equilibrium involving two highly reactive radical species, such as those in eq 1.<sup>1</sup> Nevertheless, acidities of about a dozen nitrogen and



(1) For reviews, see: Hammerich, O.; Parker, V. D. *Adv. Phys. Org. Chem.* 1984, 20, 55-189 and references cited therein.

oxygen radical cation acids have been measured, including those for  $\text{PhNH}_2^{\bullet+}$ ,<sup>2</sup>  $\text{Me}_2\text{NH}^{\bullet+}$ ,<sup>3</sup> and  $\text{PhOH}^{\bullet+}$ ,<sup>4</sup> which have  $\text{p}K_{\text{HA}^{\bullet+}}$  values of 7, 6.5-7, and -2, respectively. Typically, the radical cations were generated by photolysis or pulse radiolysis in an

(2) Land, E. J.; Porter, G. *Trans. Faraday Soc.* 1963, 59, 2027.

(3) Fessenden, R. W.; Neta, P. *J. Phys. Chem.* 1972, 76, 2857-2859.

(4) Dixon, W. T.; Murphy, D. *J. Chem. Soc., Faraday Trans. 2* 1976, 72, 1221-1230.